Comparison of several BHT correction methods: a case study on an Australian data set

Bruno Goutorbe, Francis Lucazeau, Alain Bonneville

Manuscript submitted to Geophys. J. Int.

Comparison of several BHT correction methods: a case study on an Australian data set

Bruno Goutorbe*, Francis Lucazeau and Alain Bonneville

Institut de Physique du Globe de Paris, France

**Corresponding author. E-mail: goutorbe@ipgp.jussieu.fr*

7th February 2007

SUMMARY

Bottom-hole temperatures (BHT) from oil exploration provide useful constraints on the subsurface thermal regime, but they need to be corrected to obtain the equilibrium temperature. In this work we introduce several BHT correction methods and compare them using a large Australian data set of more than 650 groups of multiple BHT measurements in about 300 oil exploration boreholes. Existing and suggested corrections are classified within a coherent framework, in which methods are divided into: line/cylinder source; instantaneous/continuous heat extraction; one/two component(s). Comparisons with reservoir test temperatures show that most of the corrections lead to reliable estimates of the formation equilibrium temperature within $\pm$ 10°C, but too few data exist to perform an inter-comparison of the models based on this criterion. As expected, the Horner method diverges from its parent models for small elapsed times (or equivalently large radii). The mathematical expression of line source models suffers from an unphysical delay time that also restrains their domain of applicability. The model that takes into account the difference of thermal properties between circulating mud and surrounding rocks – that is the two-component model – is delicate to use because of its high complexity. For these reasons, our preferred correction methods are the cylindrical source models. We show that mud circulation time below 10 hours has a negligible effect. The cylindrical source models rely on one parameter depending on the thermal diffusivity and the borehole ra-

dius, which are poorly constrained, but the induced uncertainty on the extrapolations remains reasonably low.

Key words: Borehole, Geothermics, Bottom-hole temperatures, BHT correction methods

1 INTRODUCTION

It is important in many domains to have a proper knowledge of undisturbed subsurface temperature. For example, it is used in oil exploration to constrain the temperature history of sedimentary basins in order to estimate hydrocarbon maturation. In geothermal energy, it is needed to quantify the heat content of reservoirs. In addition, the geothermal gradient must be known to estimate terrestrial heat flow, which is a fundamental parameter in Earth sciences for the study of mantle convection, lithospheric deformation, hydrothermal circulation, radiogenic heat production and cooling of the Earth. Temperatures measured in deep boreholes after drilling form a vast data set, but it is well known that they are altered by the drilling process, mainly because of the cooling effect of mud circulation. Temperature logs are usually not used because they are too perturbed by the complex drilling history. Only recordings of the bottom-hole temperature (BHT) can be corrected, and then only if an adequate time series is collected..

A multitude of methods to extrapolate the undisturbed temperature have been developed, corresponding to various assumptions about the cooling effect of the circulating mud, the borehole geometry and the thermal properties of the borehole/surrounding rock system. A review of existing corrections can be found in Hermanrud *et al.* (1990), but few studies have tried to classify and compare the methods using a large real-world BHT data set. In most of the cases, inter-comparisons were limited to a few data sets and/or a few correction methods (Hermanrud *et al.* 1990, Luheshi 1983, Shen & Beck 1986).

The aim of this paper is to describe several correction methods and compare them using a large data set of BHT measurements from Australian oil exploration wells. In the next section we gradually introduce a class of BHT corrections, namely analytical methods in which mud circulation is modelled as an infinite line or cylindrical sink of heat. New models are suggested within the framework of existing methods, which we classify by their underlying assumptions

(line/cylinder source, instantaneous/continuous heat extraction, one or two component(s)). Finally, we describe the Australian data set, apply the different methods to it, and discuss the specificities, weaknesses and domains of applicability of each method.

2 MATHEMATICAL FORM OF BHT CORRECTIONS

We develop the theoretical temperature evolution at the bottom of the borehole, predicted by the different correction methods. Parameters needed for each correction are listed in Table 1.

2.1 Line source methods

Most of the models assume that the mud circulation acts as a heat sink. An instantaneous line source/sink induces the following temperature perturbation (Carslaw & Jaeger 1959):

$$\delta T_{\text{ILS}}\left(t_e\right) = \frac{Q_{\text{ILS}}}{4\pi\kappa_r t_e} \exp\left(-\frac{r^2}{4\kappa_r t_e}\right), \tag{1}$$

where t_e is the elapsed time after heat release, r the distance to the source, κ_r the rock thermal diffusivity and Q_{ILS} the thermal strength per unit of source length, that is, the temperature to which a unit length of source would raise a unit volume of rock ($Q_{\text{ILS}} < 0$ as we consider a heat sink).

If we choose not to neglect the circulation time t_c, and consider that heat is continuously relaxed, we derive for $t < t_c$ the expression for a continuous line source by integrating Eq. (1) over time:

$$\delta T_{\text{CLS}}\left(t\right) = \int_0^t \frac{Q_{\text{CLS}}}{4\pi\kappa_r\left(t-t'\right)} \exp\left(-\frac{r^2}{4\kappa_r\left(t-t'\right)}\right) dt' \tag{2a}$$

$$= \frac{Q_{\text{CLS}}}{4\pi\kappa_r} E_1\left(\frac{r^2}{4\kappa_r t}\right), \tag{2b}$$

with Q_{CLS} the thermal strength per unit length and time of the line source and $E_1(x) = \int_x^\infty \frac{e^{-u}}{u} du$ the exponential integral. Applying the superposition principle, the temperature after the end of mud circulation is

$$\delta T_{\text{CLS}}\left(t_c, t_e\right) = \frac{Q_{\text{CLS}}}{4\pi\kappa_r}\left[E_1\left(\frac{r^2}{4\kappa_r\left(t_c+t_e\right)}\right) - E_1\left(\frac{r^2}{4\kappa_r t_e}\right)\right], \tag{3}$$

where t_e is the elapsed time since the end of mud circulation. This expression was first derived by Bullard (1947) and was used by, e.g., Funnell *et al.* (1996), Townend (1999), Zschocke (2005),

with $r = a$ (radius of the borehole). Under the assumption $a^2/4\kappa_r t_e \ll 1$, and using the following series expansion near 0:

$$E_1(x_2) - E_1(x_1) = \ln\left(\frac{x_1}{x_2}\right) + x_2 - x_1 + O(x_1^2, x_2^2), \tag{4}$$

Eq. (3) is approximated by the well-known Horner formula (Dowdle & Cobb 1975):

$$\delta T_{\text{Horn}}\,(t_c, t_e) \approx \frac{Q_{\text{CLS}}}{4\pi\kappa_r} \ln\left(1 + \frac{t_c}{t_e}\right), \tag{5}$$

which is the most widely used correction method.

If, instead of an infinite line source, one considers a more realistic semi-infinite problem, it is easy to show from symmetry considerations that Eqs. (1), (3) and (5) still hold to a factor $\frac{1}{2}$ on the plane located at the end of the line and perpendicular to it.

2.2 Cylinder source methods

We now turn to the cases where the borehole radius a is not neglected. At the centre of the borehole, the effect of an instantaneous cylinder source can be found by integrating Eq. (1) over the radius:

$$\delta T_{\text{ICS}}(t_e) = \int_0^a \frac{Q_{\text{ICS}}}{4\pi\kappa_r t_e} \exp\left(-\frac{r^2}{4\kappa_r t_e}\right) 2\pi r dr \tag{6a}$$

$$= Q_{\text{ICS}} \left[1 - \exp\left(-\frac{a^2}{4\kappa_r t_e}\right)\right], \tag{6b}$$

where Q_{ICS} is the thermal strength per unit volume of source, which is simply the initial temperature perturbation in the cylinder. This solution was introduced by Leblanc *et al.* (1981) and Middleton (1982). Taking into account the circulation time, t_c, we derive for $t < t_c$ the continuous cylinder source expression (still at the centre of the borehole) by integrating Eq. (6) over time:

$$\delta T_{\text{CCS}}(t) = \int_0^t Q_{\text{CCS}} \left[1 - \exp\left(-\frac{a^2}{4\kappa_r\,(t - t')}\right)\right] dt' \tag{7a}$$

$$= Q_{\text{CCS}} \cdot t - \frac{Q_{\text{CCS}} \cdot a^2}{4\kappa_r} E_2\left(\frac{a^2}{4\kappa_r t}\right), \tag{7b}$$

with Q_{CCS} the thermal strength per unit volume and time of source, and $E_2(x) = \int_x^\infty \frac{e^{-u}}{u^2} du$ the second-order exponential integral. Applying the superposition principle, after the end of mud

circulation:

$$\delta T_{\text{CCS}}(t_c, t_e) = Q_{\text{CCS}} \cdot t_c - \frac{Q_{\text{CCS}} \cdot a^2}{4\kappa_r} \left[E_2\left(\frac{a^2}{4\kappa_r\left(t_c + t_e\right)}\right) - E_2\left(\frac{a^2}{4\kappa_r t_e}\right)\right]. \tag{8}$$

Again, using the series expansion near 0:

$$E_2(x_2) - E_2(x_1) = \frac{1}{x_2} - \frac{1}{x_1} + \ln\left(\frac{x_2}{x_1}\right) + \frac{x_1 - x_2}{2} + O(x_1^2, x_2^2) \tag{9}$$

and the identity $Q_{\text{CLS}} \Leftrightarrow Q_{\text{CCS}} \cdot \pi a^2$, the first non-null terms of the series expansions of the CCS [Eq. (8)] and CLS [Eq. (3)] corrections, as $a^2/4\kappa_r t_e \to 0$, are equal and correspond to the Horner approximation [Eq. (5)]. However, the next terms differ, showing that the line source model is not a higher-order approximation of the cylinder source method.

As in the line source case, Eqs. (6) and (8) just have to be divided by two in the semi-infinite case, as the observation point is at the bottom of the borehole.

2.3 Two-component model

A more complex model, which takes into account the difference in thermal properties between the borehole mud and the surrounding rocks, was studied by Luheshi (1983), using numerical methods. Shen & Beck (1986) proposed analytical solutions for this problem based on Laplace transforms. We define some dimensionless parameters:

$$\tau_e = \frac{\kappa_r t_e}{a^2}, \quad \tau_c = \frac{\kappa_r t_c}{a^2}, \quad \beta = \frac{\rho c_m}{\rho c_r}, \quad \delta = \sqrt{\frac{\kappa_m}{\kappa_r}}, \quad \sigma = \frac{\lambda_m}{\lambda_r}\sqrt{\frac{\kappa_r}{\kappa_m}}, \quad R = \frac{r}{a} \tag{10}$$

where the subscripts m and r refer respectively to mud and rock properties, ρc is the volume heat capacity and λ the thermal conductivity (the other symbols are identical to previous sections). Assuming that mud circulates at constant temperature, Shen & Beck (1986) show that the temperature perturbation takes the form:

$$\frac{\delta T_{\text{2-comp}}(\tau_c, \tau_e)}{\Delta T_0} = 1 - \frac{4}{\pi^2}\int_{w=0}^{\infty} \frac{J_0\left(\frac{w}{\delta}\right) J_0\left(R\frac{w}{\delta}\right)}{\phi^2(w) + \psi^2(w)} G_1(\tau_c, \tau_e, w)\,\frac{dw}{w}, \tag{11a}$$

$$\text{with } G_1(\tau_c, \tau_e, w) = \frac{4}{\pi^2}\int_{u=0}^{\infty} \frac{e^{-w^2\tau_e} - e^{-u^2\tau_e}}{u^2 - w^2} \frac{e^{-u^2\tau_c}}{J_0^2(u) + Y_0^2(u)}\frac{du}{u}, \tag{11b}$$

$$\phi(w) = \sigma Y_0(w) J_1\left(\frac{w}{\delta}\right) - Y_1(w) J_0\left(\frac{w}{\delta}\right), \tag{11c}$$

$$\psi(w) = \sigma J_0(w) J_1\left(\frac{w}{\delta}\right) - J_1(w) J_0\left(\frac{w}{\delta}\right), \tag{11d}$$

with ΔT_0 the initial difference of temperature between the mud and rock and J_i, Y_i the Bessel functions of the first and second kind. If, on the other hand, mud circulation is modelled as a constant heat sink per unit time and length $Q_{\text{2-comp}}$ (< 0), then:

$$\frac{\lambda_r}{Q_{\text{2-comp}}}\delta T_{\text{2-comp}}(\tau_c, \tau_e) = H(\tau_c + \tau_e) - H(\tau_e) - \frac{2}{\pi^3}\int_{w=0}^{\infty} \frac{\left[\frac{\beta}{2}J_0\left(\frac{w}{\delta}\right) - \frac{\sigma}{w}J_1\left(\frac{w}{\delta}\right)\right] J_0\left(R\frac{w}{\delta}\right)}{\phi^2(w) + \psi^2(w)} G_2(\tau_c, \tau_e, w)\frac{dw}{w}, \tag{12a}$$

$$\text{with } G_2(\tau_c, \tau_e, w) = \frac{4}{\pi^2}\int_{u=0}^{\infty} \frac{e^{-w^2\tau_e} - e^{-u^2\tau_e}}{u^2 - w^2}\frac{1 - e^{-u^2\tau_c}}{\phi_\infty^2(u) + \psi_\infty^2(u)}\frac{du}{u}, \tag{12b}$$

$$H(\tau) = \frac{1}{\pi^2}\int_{u=0}^{\infty} \frac{1 - e^{-u^2\tau}}{u^2}\frac{J_0(Ru)\,\phi_\infty(u) - Y_0(Ru)\,\psi_\infty(u)}{\phi_\infty^2(u) + \psi_\infty^2(u)}du, \tag{12c}$$

$$\phi_\infty(u) = \frac{\beta u}{2}Y_0(u) - Y_1(u), \tag{12d}$$

$$\psi_\infty(u) = \frac{\beta u}{2}J_0(u) - J_1(u). \tag{12e}$$

As for the line source method, the above formulae are used with $r = a$ $(R = 1)$ for BHT correction.

3 APPLICATION TO THE AUSTRALIAN TEMPERATURE SET

3.1 Data set and methodology

We had access to oil exploration data in $\sim$ 300 wells from Wiltshire Geological Services®. Most of the wells are located in Australia and a few in New-Zealand (Fig. 1). The data set accounts for about 650 groups of multiple $\{T_{\text{BHT}}, t_e\}$ measurements, a part of them also having the circulation time t_c (we take a default value t_c of 3 hours for the others). Half of the groups are made of two measurements, one-third of three measurements, and the rest of four or more. There are also complete sets of geophysical well logs – including caliper, sonic, density, neutron, electrical resistivity and gamma-ray. Finally, around 100 temperatures T_{DST} from drillstem tests are available from 18 of the wells. T_{DST} corresponds to the reservoir fluid temperature, which is supposed to be in equilibrium with surrounding rocks, so it is considered to represent the undisturbed rock temperature. All available temperature data are shown in Fig. 2.

Since a BHT is a perturbed measurement, $T_{\text{BHT}} = T_\infty + \delta T([t_c,]t_e)$ with T_∞ the undisturbed

rock temperature to estimate and δT the chosen model in the list of Table 1. To our knowledge, the ILS and CCS corrections have never been presented, but as they appear naturally within the framework, we shall keep them in the following inter-comparison. The parameters Q and ΔT_0 (see previous section) are considered to be unknown, so at least two $T_{\rm BHT}$ and their elapsed time t_e must be available to extrapolate T_∞, which we do using a classical least-square linear regression. Extrapolations that yield Q or $\Delta T_0 > 0$ (that is, a T_∞ lower than BHT measurements) are discarded.

The other parameters (Table 1) are estimated with the help of the geophysical well logs. The radius a is available from the caliper log after some smoothing. Unlike usual approaches, we do not assign a constant thermal diffusivity to the rocks, as it depends on the in situ temperature, porosity and rock type. The rock thermal conductivity λ_r is predicted from the well logs (sonic, density, neutron, electrical resistivity and gamma-ray) using a recently developed neural network method (Goutorbe *et al.* 2006). The volume heat capacity of the rock matrix ρc_{matrix} hardly varies from one rock type to another (Beck 1988) and depends on the temperature T. The rock heat capacity ρc_r is the harmonic mean of $\rho c_{matrix}(T)$ and the heat capacity of water $\rho c_{water}(T)$, weighted with volume proportions. $\rho c_{matrix}(T)$ is inferred from Vosteen & Schellschmidt (2003), $\rho c_{water}(T)$ from Lide (2004). The volume proportions are calculated from the neutron porosity log. T is actually the T_∞ we seek, but as temperature only has a second-order effect on heat capacity, a rough estimate is sufficient: we do this by adding to each $T_{\rm BHT}$ measured at depth $z_{\rm BHT}$ the quantity $\widehat{T}_{\rm DST}(z_{\rm BHT}) - \widehat{T}_{\rm BHT}(z_{\rm BHT})$, where $\widehat{T}_{\rm DST}(.)$ and $\widehat{T}_{\rm BHT}(.)$ denote respectively the linear regression of all $T_{\rm DST}$ and all $T_{\rm BHT}$ against their depth of measurement. Rock thermal diffusivity is then $\kappa_r = \lambda_r / \rho c_r$. The mean values of λ_r, ρc_r and κ_r in our data set are:

$$\lambda_r = 1.9 \pm 0.6 \text{ W.m}^{-1}\text{.K}^{-1}, \tag{13a}$$

$$\rho c_r = 3 \pm 0.2 \cdot 10^6 \text{ J.K}^{-1}\text{.m}^{-3}, \tag{13b}$$

$$\kappa_r = 6.8 \pm 2 \cdot 10^{-7} \text{ m}^2\text{.s}^{-1}. \tag{13c}$$

Circulating mud properties obviously vary depending on mud type and operating conditions, however due to lack of information it is difficult to have proper estimates. Hence as a crude ap-

proximation we have taken constant values, suggested by Luheshi (1983):

$$\lambda_m = 0.7 \text{ W.m}^{-1}\text{.K}^{-1}, \tag{14a}$$

$$\rho c_m = 5 \cdot 10^6 \text{ J.K}^{-1}\text{.m}^{-3}, \tag{14b}$$

$$\kappa_m = \frac{\lambda_m}{\rho c_m} = 1.4 \cdot 10^{-7} \text{ m}^2\text{.s}^{-1}. \tag{14c}$$

3.2 Results

3.2.1 T_∞ *versus* T_{DST}

As T_{DST} are supposed to be undisturbed rocks temperatures (see previous section) we compared them with T_∞ resulting from correction of BHT measurements, in wells where both types of temperature are available (Fig. 3). Too few data exist to perform quantitative statistics, and comparison is difficult as temperatures are usually not at same depths, therefore only qualitative remarks can be made. In most of the wells, the results are quite close from each other, except for the two-component model which seems to give systematically higher predictions, and a few corrected temperatures using the line-source models that are clearly out of tendency. T_∞ are usually in agreement with the T_{DST} geotherm within $\pm$5-10°C, which is the accuracy expected by a number of authors (e.g. Brigaud 1989). In wells showing inconsistencies (e.g., well Montague 1), no model is in agreement with the T_{DST} geotherm, which questions the quality of T_{BHT} or T_{DST} measurements rather than the correction methods. In well Wanaea 1, below the only T_{DST} measurement, the temperatures corrected with the two-component model seem to be in better agreement with T_{DST} than the other corrections. However the discrepancy of the two-component model predictions with respect to the other corrections, and also with respect to the other predictions from the same correction at lower depths, tend to suggest that the T_{DST} measurement is the one questionable. Hence from these comparisons it is difficult to establish a rating of the different correction methods, but it can be seen that in most cases they give “reasonable” predictions.

3.2.2 Horner versus CLS/CCS

The Horner model is the first order development of CLS and CCS corrections to the limit $a^2/4\kappa t_e \to 0$ (see section 2.1). As expected, Horner predictions of T_∞ diverge from its "parents" models when the underlying approximation do not hold any more (Fig. 4), Horner extrapolations being systematically lower. Therefore, as discussed by several authors (e.g., Shen & Beck 1986), one should avoid the use of Horner correction when $a^2/4\kappa t_e \gtrsim 1$ (too large radius or, equivalently, too small elapsed time).

3.2.3 Line source versus cylinder source

As pointed out by Luheshi (1983), when the effect of the mud is modelled as a line source, the borehole radius is taken into account by considering the perturbation at the distance $r = a$ of the line (see section 2.1). As a consequence the mathematical form of the thermal evolution (Eqs. 1 and 3) predicts that the temperature continues to decrease after the end of mud circulation (Fig. 5a), as some time is necessary for heat to propagate to the distance $r = a$ from the line source. This theoretical "delay time" t_d is obviously unphysical, as one expects borehole temperature to increase immediately after the end of mud circulation. If a T_{BHT} in a group has an associated elapsed time t_e that is lower than t_d (thus supposedly belonging to the decreasing part of the thermal evolution), then the model predicts a completely unrealistic T_∞ (see example in Fig. 5a). Therefore the line source methods cannot be used on T_{BHT} having $t_e < t_d$. By solving the equations $\left.\frac{\partial \delta T_{\text{ILS}}}{\partial t_e}\right|_{t_e=t_d} = 0$ and $\left.\frac{\partial \delta T_{\text{CLS}}}{\partial t_e}\right|_{t_e=t_d} = 0$, it is easy to see that $t_d = a^2/4\kappa_r$ for the ILS model, and numerical resolution shows that $t_d \sim a^2/4\kappa_r$ for the CLS correction if t_c is not too large (Fig. 5b). So the line source methods cannot be applied when:

$$t_e < t_d, \tag{15a}$$

$$\text{that is } \frac{a^2}{4\kappa_r t_e} > 1, \tag{15b}$$

which is confirmed by the large discrepancy between line source and cylinder source models as $a^2/4\kappa_r t_e \gtrsim 1$ (Fig. 5c). Therefore our conclusion is that the line source models do not necessarily have a larger applicability domain than the Horner correction.

3.2.4 Instantaneous source versus continuous source

Forward modelling has shown that the circulation time t_c has a non negligible influence on the theoretical temperature perturbation δT (e.g., Luheshi 1983). However, the opposite is not necessarily true, i.e., t_c may not have such an influence when extrapolating T_∞ from T_{BHT} measurements – as noticed by, e.g., Funnell *et al.* (1996). On our data, differences between continuous and instantaneous corrections are usually not larger than a few percent for $t_c < 10$ hours (Fig. 6). Beyond 10 hours, t_c seems to have more effect on the predictions, at least for the cylinder source models, but too few data are available to draw a firm conclusion.

3.2.5 Two-component model versus cylinder source models

As pointed out by Shen & Beck (1986), the constant temperature and constant heat supply versions of the two-component model give virtually identical results in practical applications (Fig. 7a). On the other hand, the two-component model extrapolate equilibrium temperatures that are largely higher than the other corrections (Fig. 7b). Such discrepancies are puzzling, and close inspection shows that the two-component model often extrapolate unrealistic values of T_∞, as this can be seen on the examples of Fig. 7c. Hence, although the theoretical background of the method is certainly more accurate, its complexity and the number of parameters to estimate may actually make it less robust on real-world cases.

3.2.6 Sensitivity with respect to $r^2/4\kappa_r$

As can be seen in Eqs. (1), (3), (6) and (8), the main parameter of the line and cylinder source models is $\tau \equiv a^2/4\kappa_r$. As we have only indirect estimations, it is important to quantify the sensitivity of the extrapolations with respect to τ. The relative uncertainty on τ is

$$\frac{\delta\tau}{\tau} = \sqrt{\left(2\frac{\delta a}{a}\right)^2 + \left(\frac{\delta\kappa_r}{\kappa_r}\right)^2}. \tag{16}$$

Assuming that a is relatively well constrained thanks to direct log measurement ($\delta a/a \sim$ 5-10%) and the indirect estimate of κ_r much less reliable ($\delta\kappa_r/\kappa_r \sim$ 15-25%), we have $\delta\tau/\tau \sim$ 15-30%. This generates in turn some variability on the extrapolated T_∞. The sensitivity increases with τ,

staying in most cases below $\pm 3\%$ for a relative uncertainty on τ of 15%, and reaching $\pm 5\%$ with $\delta\tau/\tau = 30\%$ (Fig. 8). Therefore it seems that the sensitivity of the corrections remains reasonably low, even with thermal diffusivity κ_r poorly constrained.

4 SUMMARY AND CONCLUSIONS

We have presented and classified several analytical BHT corrections of various complexity levels. By performing inter-comparisons on a real-world oil exploration data set from Australia, we have drawn the following conclusions:

(1) Extrapolated undisturbed temperatures from all methods are qualitatively in agreement with measurements from drillstem tests (within 5-10°C) in most of the wells.

(2) As expected, the widely used Horner method breaks down when its underlying assumption ($a^2/4\kappa_r t_e \ll 1$) is not valid.

(3) The line source models, which are sometimes used instead of the Horner method, suffer from an unphysical delay time that actually restrain their applicability domain.

(4) It seems that the circulation time cannot be neglected beyond 10 hours, at least for the cylinder models, but this conclusion does not lie on a firm statistical basis.

(5) Taking into account the contrast of thermal properties between circulating mud and surrounding rocks is the most realistic way of modelling the problem. However the mathematical form of the correction reaches a level of complexity, and requires a large number of parameters, making it delicate to use on practical cases.

The domains of applicability of the correction methods are summarized in Table 2. The cylinder source models are our preferred corrections, as they take into account some geometrical and thermal characteristics of the circulation process, have few theoretical restrictions regarding their applicability domain and keep a simple analytical form for practical use.

5 ACKNOWLEDGEMENTS

Michael Wiltshire, the director of the company Wiltshire Geological Services®, provided us oil exploration data from Australia, making this work possible.

References

Beck, A., 1988. Methods for determining thermal conductivity and thermal diffusivity, in *Handbook of terrestrial heat-flow density determination*, edited by R. Haenel, L. Rybach, & L. Stegena, Kluwer Academic Publishers.

Brigaud, F., 1989. *Conductivité thermique et champ de température dans les bassins sédimentaires à partir des données de puits*, Ph.D. thesis, Centre Géologique et Géophysique, Université des Sciences et Techniques du Languedoc, Montpellier, France, 414 p.

Bullard, E., 1947. The time taken for a borehole to attain temperature equilibrium, *Mon. Not. R. Astron. Soc.*, **Geophys. Suppl. 5**, 127–130.

Carslaw, H. & Jaeger, J., 1959. *Conduction of heat in solids*, Clarendon, Oxford, 510 p.

Cramer, W. & Leemans, R., pers. comm. The climate database version 2.1, available from World Wide Web: http://portal.pik-potsdam.de/members/cramer/climate.html.

Dowdle, W. L. & Cobb, W., 1975. Static formation temperature from well logs – an empirical method, *J. Petr. Tech.*, pp. 1326–1330.

Funnell, R., Chapman, D., Allis, R., & Armstrong, P., 1996. Thermal state of the Taranaki Basin, New Zealand, *J. Geophys. Res.*, **101**(B11), 25197–25215.

Goutorbe, B., Lucazeau, F., & Bonneville, A., 2006. Using neural networks to predict thermal conductivity from geophysical well logs, *Geophys. J. Int.*, **166**, 115–125, doi: 10.1111/j.1365-246X.2006.02924.x.

Hermanrud, C., Cao, S., & Lerche, I., 1990. Estimates of virgin rock temperature derived from BHT measurements: Bias and error, *Geophysics*, **55**(7), 924–931.

Leblanc, V., Pascoe, L., & Jones, F., 1981. The temperature stabilization of a borehole, *Geophysics*, **46**(9).

Levitus, S. & Boyer, T., 1994. World Ocean Atlas 1994, Volume 4: Temperature, NOAA ATLAS NESDIS 4.

Lide, D., 2004. *CRC Handbook of chemistry and physics*, 85^{th} *Edition*, CRC Press.

Luheshi, M., 1983. Estimation of formation temperature from borehole measurements, *Geophys. J. R. Astr. Soc.*, **74**, 747–776.

Middleton, M., 1982. Bottom-hole temperature stabilization with continued circulation of drilling mud, *Geophysics*, **47**(12), 1716–1723.

Shen, P. & Beck, A., 1986. Stabilization of bottom-hole temperature with finite circulation time and fluid flow, *Geophys. J. R. Astr. Soc.*, **86**, 63–90.

Townend, J., 1999. Heat flow through the West Coast, South Island, New Zealand, *New Zeal. J. Geol. Geophys.*, **42**, 21–31.

Vosteen, H. & Schellschmidt, R., 2003. Influence of temperature on thermal conductivity, thermal capacity and thermal diffusivity for different types of rock, *Phys. Chem. Earth*, **28**, 499–509.

Zschocke, A., 2005. Correction of non-equilibrated temperature logs and implications for geothermal investigations, *J. Geophys. Eng.*, **2**, 364–371, doi: 10.1088/1742-2132/2/4/S10.

LIST OF FIGURES

Table 1. List of parameters needed for BHT corrections (ILS: instantaneous line source; CLS: continuous line source; ICS: instantaneous cylinder source; CCS: continuous cylinder source; 2-comp: two-component).

Par.	Description	Horner	ILS	CLS	ICS	CCS	2-comp
t_c	Mud circulation time	$\times$		$\times$		$\times$	$\times$
a	Borehole radius		$\times$	$\times$	$\times$	$\times$	$\times$
κ_r	Rock thermal diffusivity		$\times$	$\times$	$\times$	$\times$	$\times$
λ_r	Rock thermal conductivity						$\times$
ρc_r	Rock vol. heat capacity						$\times$
κ_m	Mud thermal diffusivity						$\times$
λ_m	Mud thermal conductivity						$\times$
ρc_m	Mud vol. heat capacity						$\times$

Table 2. Summary of the restrictions for the correction methods. The two-component model has not been included because its complexity is a serious obstacle to its use.

Correction	Restrictions
Horner	$a^2/4\kappa t_e \ll 1$
ILS	$a^2/4\kappa t_e < 1$
CLS	$a^2/4\kappa t_e < 1$
ICS	$t_c < 10$ hours?
CCS	$-$

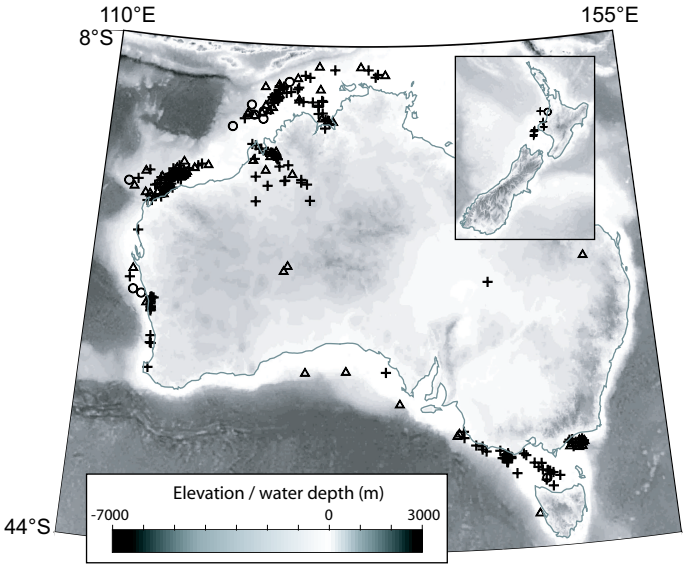

Figure 1. Location of oil exploration wells in which temperature data are available. Crosses: wells having one or two groups of multiple BHT measurements; open triangles: three or four groups; open circles: five groups or more.

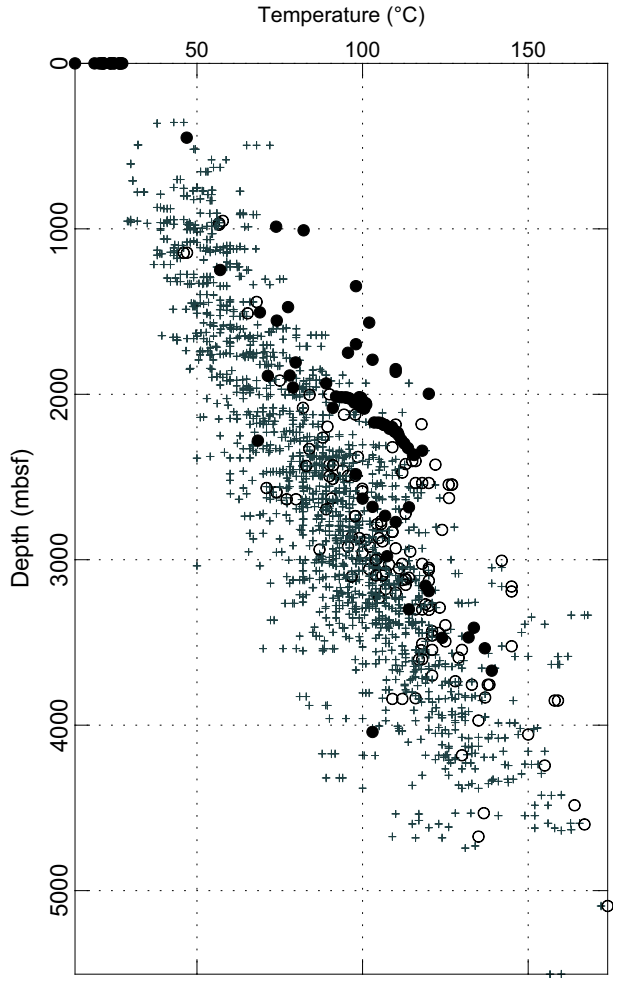

Figure 2. Available temperature measurements versus depth. T_{BHT}: grey crosses ($t_e < 30$ hours) and open circles ($t_e \geq 30$ hours); T_{DST} and surface temperatures: black dots. Surface temperatures from Levitus & Boyer (1994) (offshore) and Cramer & Leemans (pers. comm.) (onshore) databases. As can be expected, the geotherm defined by BHT measurements with a high elapsed time t_e is closer to the T_{DST} geotherm.

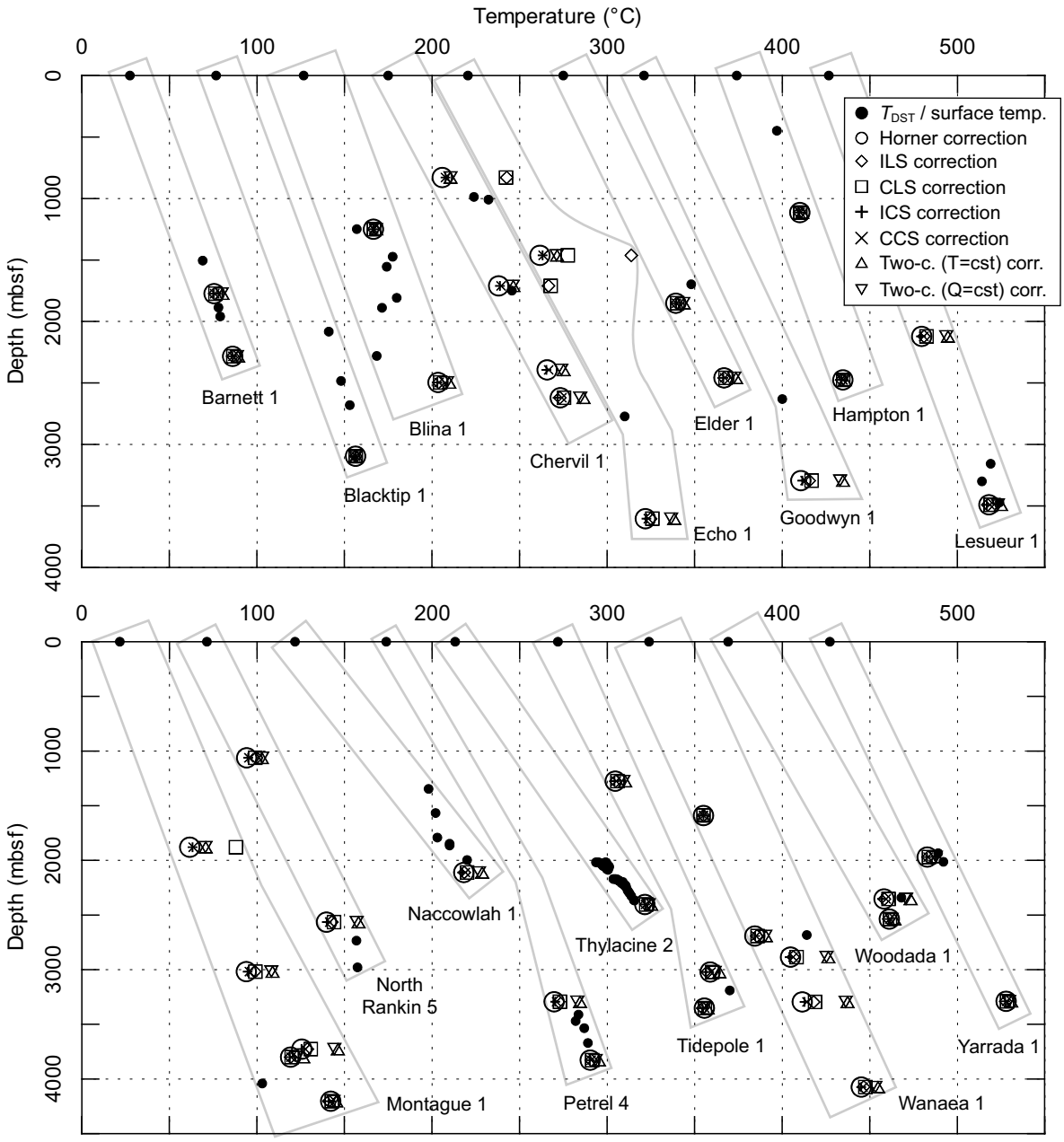

Figure 3. Surface temperatures, T_{DST} and T_∞ (from correction of T_{BHT}) versus depth, in wells where both T_{BHT} and T_{DST} are available. Temperatures of a given well are shifted of $+50$°C with respect to previous well. The size of symbols for T_∞ corresponds roughly to an uncertainty of ± 5°C. The two versions of the two-component model correspond respectively to the constant temperature and constant supply of heat assumptions (see section 2.3). At some depths there are missing methods, as they yielded Q or $\Delta T_0 > 0$ (see section 3.1).

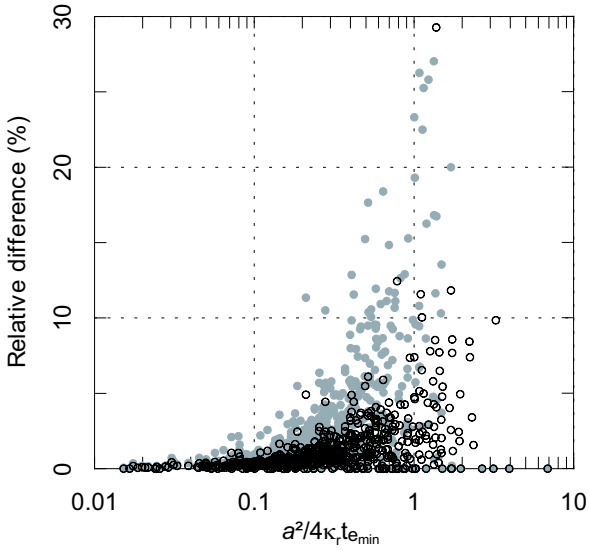

Figure 4. Relative differences of predicted T_∞ between: CLS and Horner corrections (grey dots), CCS and Horner corrections (open circles), versus $a^2/4\kappa_r t_e$ (with smallest t_e of the T_{BHT} series taken).

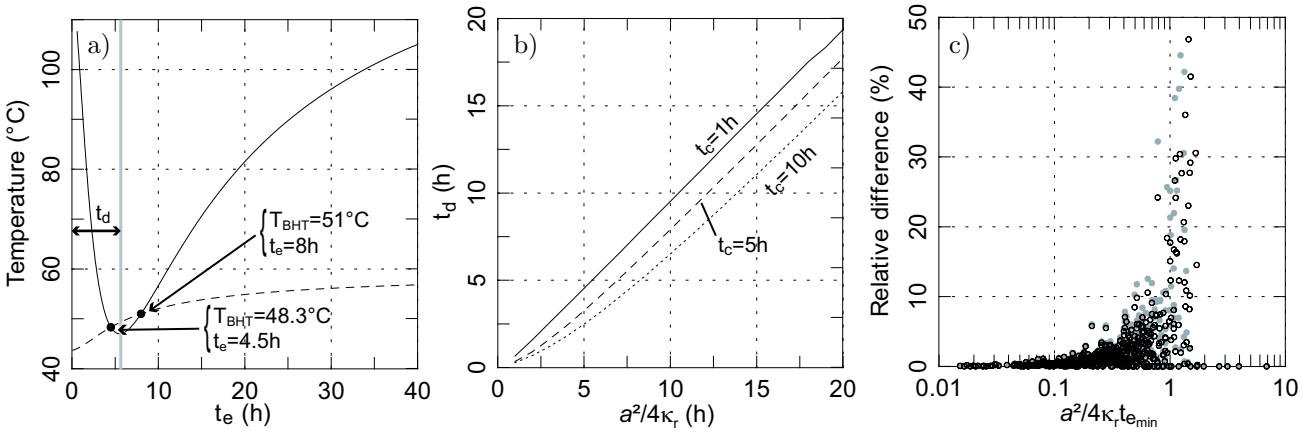

Figure 5. (a) Example of T_∞ extrapolation from a couple of T_{BHT} measurements (black dots) taken from well Bridgewater Bay 1. $t_c = 3$ hours, $a = 0.21$ m, $\kappa_r = 4.49 \cdot 10^{-7}$ m^2.s^{-1}. The CLS model (solid line) predicts an unrealistic $T_\infty = 141$°C, while the CCS model (dashed line) predicts $T_\infty = 59$°C. (b) Delay time t_d of the CLS model as a function of $a^2/4\kappa_r$, for various t_c. (c) Relative differences of predicted T_∞ between: ILS and ICS corrections (grey dots), CLS and CCS corrections (open circles), versus $a^2/4\kappa_r t_e$ (with smallest t_e of the T_{BHT} series taken).

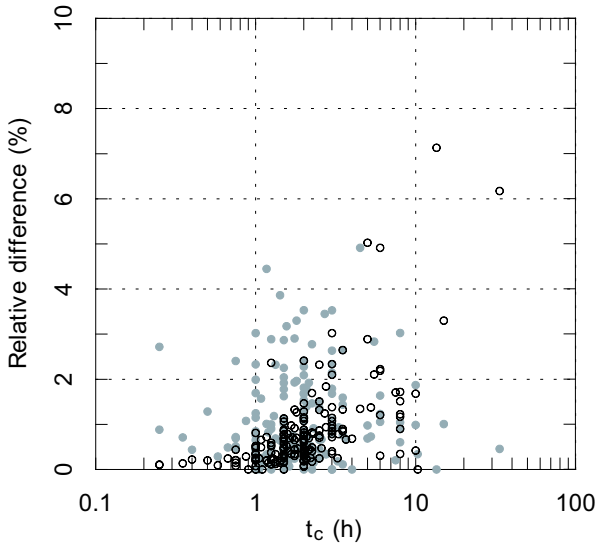

Figure 6. Relative differences of predicted T_∞ between: CLS and ILS corrections (grey dots), CCS and ICS corrections (open circles), versus mud circulation time t_c. There are less data than other comparisons because we have only considered temperatures with available t_c.

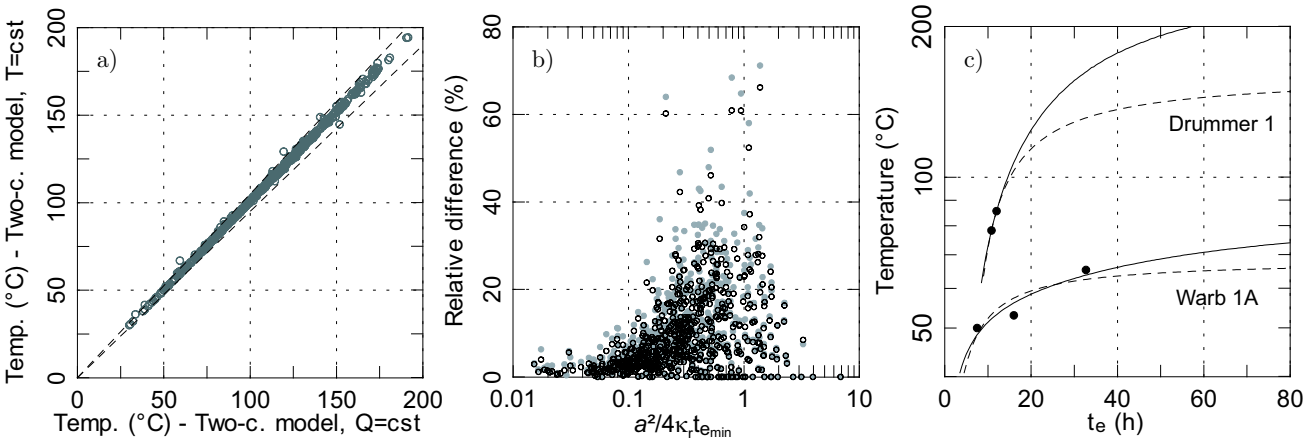

Figure 7. (a) T_∞ from the constant temperature version versus T_∞ from the constant supply of heat version of the two-component model (open circles), with $\pm 5\%$ relative difference shown (dashed lines); (b) Relative differences of predicted T_∞ between: two-component and ICS corrections (grey dots), two-component and CCS corrections (open circles), versus $a^2/4\kappa_r t_e$ (with smallest t_e of the $T_{\rm BHT}$ series taken); (c) Example of T_∞ extrapolation from series of $T_{\rm BHT}$ measurements (black dots) taken from wells Drummer 1 and Warb 1A. Parameters for Drummer 1: $t_c = 1.25$ hours, $a = 0.16$ m, $\lambda_r = 2.16$ W.m.$^{-1}$.K^{-1}, $\rho c_r = 2.8 \cdot 10^6$ J.m^{-3}.K^{-1}, $\kappa_r = 7.8 \cdot 10^{-7}$ m^2.s^{-1}. Parameters for Warb 1A: $t_c = 2.5$ hours, $a = 0.23$ m, $\lambda_r = 2.22$ W.m.$^{-1}$.K^{-1}, $\rho c_r = 2.9 \cdot 10^6$ J.m^{-3}.K^{-1}, $\kappa_r = 7.7 \cdot 10^{-7}$ m^2.s^{-1}. The two-component model (solid lines) predicts unrealistic T_∞ of 266°C for Drummer 1 ($\approx T_{\rm BHT} + 180$°C!) and 89°C for Warb 1A (though last measured $T_{\rm BHT} = 65$°C with $t_e \gg t_c$), while the ICS model (dashed lines) predicts respectively $T_\infty = 161$°C and 68°C.

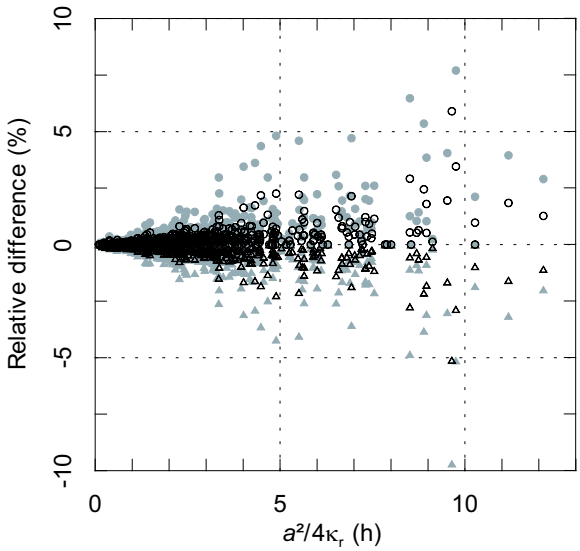

Figure 8. Relative differences between predictions with modified τ (say, τ') and initial τ, versus initial τ, using ICS model. Filled triangles: $\tau' = 0.7\tau$; filled triangles: $\tau' = 0.85\tau$; open circles: $\tau' = 1.15\tau$; open circles: $\tau' = 1.30\tau$. The sensitivity of the other models (line and cylinder source) is similar.